

The CD14^{+low}CD16⁺ monocyte subset is more susceptible to spontaneous and oxidant-induced apoptosis than the CD14⁺CD16⁻ subset

C Zhao¹, Y-C Tan¹, W-C Wong², X Sem¹, H Zhang³, H Han², S-M Ong¹, K-L Wong¹, W-H Yeap¹, S-K Sze³, P Kourilsky¹ and S-C Wong^{*1}

Human monocytes can be classified into two subsets with distinctive characteristics. In this study, we report a difference in apoptotic potential between these two subsets with CD14^{+low}CD16⁺ monocytes being more susceptible than CD14⁺CD16⁻ monocytes to undergo spontaneous apoptosis and apoptosis induced by reactive oxygen species (ROS). By global transcriptomic and proteomic approaches, we observed that CD14^{+low}CD16⁺ monocytes expressed higher levels of pro-apoptotic genes and proteins such as TNF α , caspase 3, Bax and cytochrome *c* and showed more caspases 3 and 7 activities. They also exhibited greater aerobic respiration resulting in a higher production of ROS from the mitochondria. CD14⁺CD16⁻ monocytes, in contrast, showed higher expression of glutathione (GSH)-metabolizing genes such as GSH peroxidase and microsomal GSH S-transferase and were more resistant to oxidative stress than CD14^{+low}CD16⁺ monocytes. The apoptosis of CD14^{+low}CD16⁺ monocytes was ROS dependent as reducing ROS levels significantly reduced cell death. This is the first report of a differential apoptotic propensity of human monocyte subsets, and gaining a better understanding of this process may help to provide a better understanding of the roles of these subsets during homeostasis and under pathological conditions, particularly in situations in which high levels of oxidants are present.

Cell Death and Disease (2010) 1, e95; doi:10.1038/cddis.2010.69; published online 4 November 2010

Subject Category: Immunity

Monocytes are generated in the bone marrow and serve to replenish dying resident tissue macrophages during steady state.¹ As tissue macrophages are relatively long lived, monocytes generated in the bone marrow generally far exceed the numbers required to replenish dying tissue macrophages. Hence, monocytes will remain in the blood for up to 3 days before spontaneously undergoing apoptosis.^{2,3}

Apoptosis is an important mechanism for regulating the numbers of immune cells. Monocyte culture *in vitro* in the absence of serum or activating factors will die spontaneously, which can be blocked with neutralizing antibodies (Abs) to Fas or FasL.⁴ Both reactive oxygen species (ROS) and caspases have been implicated in Fas-mediated cell death both in monocytes and in other cell types.^{5,6} The role of ROS in mediating cell death has been well documented. It is elevated in cells undergoing apoptosis⁷ and can induce apoptosis in many different cell types.⁶ Blocking ROS with anti-oxidants also inhibits apoptosis.⁵ ROS can promote cell death by inducing mitochondrial dysfunction through Bax translocation, release of cytochrome *c* and activation of caspases.⁸ Besides ROS introduced exogenously, intracellular ROS have also been accepted as a conserved apoptotic signal. In fact, the mitochondria actively and continuously generate ROS during aerobic respiration.⁹ Apart from aerobic respiration, depletion

in glutathione (GSH) pools can also result in an concomitant increase in intracellular ROS during apoptosis.¹⁰

Blood monocytes are heterogeneous and can be broadly classified into two main subsets, CD14⁺CD16⁻ (hereafter designated as CD16⁻) and CD14^{+low}CD16⁺ (hereafter CD16⁺) in humans;¹¹ and Gr1⁺CX₃CR1^{low} (hereafter Gr1⁺) and GR1⁻CX₃CR1^{hi} (hereafter Gr1⁻) in mice.¹² These subsets exhibit distinct phenotypes with respect to the expression of surface markers,^{11,13} as well as functions like migration ability and differentiation potential.¹² Interestingly, several groups have observed the differential propensity of murine monocyte subsets to undergo apoptosis in a transgenic mouse model, whereby Gr1⁻ monocytes fail to persist.^{12,14,15} In humans, CD16⁺ monocytes were observed to significantly expand in numbers under numerous inflammatory conditions such as sepsis,¹⁶ HIV infections¹⁷ and autoimmune disorders,^{18,19} which may be attributed to enhanced survival.^{3,20}

We observed from transcriptomics and proteomics data an apoptotic signature, indicating CD16⁺ monocytes to harbor a greater propensity to undergo apoptosis. Although there are data suggesting a differential apoptotic potential between murine monocyte subsets as discussed above, no similar data in human monocyte subsets have been reported. We showed in this study that CD16⁺ monocytes exhibit higher aerobic

¹Singapore Immunology Network (SIgN), Agency for Science, Technology and Research (ASTAR), 8A Biomedical Grove, Biopolis, Singapore; ²Protein Sequence Analysis Group, Biomolecular Function Discovery Division, Bioinformatic Institutes (BI), ASTAR, 30 Biopolis Street, Biopolis, Singapore and ³School of Biological Sciences, Nanyang Technological University, 60 Nanyang Drive, Singapore

*Corresponding author: S-C Wong, Infection and Immunity, Singapore Immunology Network (SIgN), Agency for Science, Technology and Research (ASTAR), 8A Medical Grove, # 04-04, Immunos, Biopolis, Singapore 138648. Tel: + 65 6407 0030; Fax: + 65 6464 2057; E-mail: wong_siew_cheng@immunol.a-star.edu.sg

Keywords: proteomics; transcriptomics; apoptosis; monocyte subsets; reactive oxygen species; anti-oxidation

Abbreviations: ROS, reactive oxygen species; GSH, glutathione; H₂O₂, hydrogen peroxide; GPX1, glutathione peroxidase 1; MGST1, microsomal glutathione S-transferase 1; NAC, N-acetyl-cysteine

Received 01.6.10; revised 23.8.10; accepted 24.9.10; Edited by P Salomoni

respiration and express lower levels of anti-oxidant genes, implying that these cells are experiencing oxidative stress. Hence, they have a greater tendency to spontaneously undergo apoptosis. Gaining a better understanding of the mechanisms involved in the differential apoptotic potential of these subsets will help shed light on their roles during homeostasis and under inflammatory conditions, particularly in situations in which high levels of oxidants are present.

Results

Identification of differentially expressed transcripts and proteins between monocyte subsets. Two human blood monocyte subsets, CD16⁺ and CD16⁻, were routinely purified from peripheral blood mononuclear cells (PBMCs) to a purity of >95% (Figure 1). For transcriptomics, experiments were performed separately using samples obtained from four different individuals. For proteomics, experiments were performed using samples pooled from three different individuals and run three times on the QSTAR (Applied Biosystems; MDSSciex, Foster City, CA, USA) and once on the LTQ-Orbitrap (ThermoFinnigan, San Jose, CA, USA) mass spectrometers. Samples were pooled for proteomics because of the limited numbers of CD16⁺ monocytes obtained from an individual sample. The samples used for transcriptomics and proteomics were different. By transcriptomics analysis, 10 982 out of 48 701 transcript targets available on the Illumina microarray (Illumina, San Diego, CA, USA) were reliably identified for both monocyte subsets and used for determining differentially expressed

transcripts. Using a fold change of ≥ 2 between monocyte subsets as the cutoff criterion, 520 differentially expressed transcripts were identified (Figure 1a). By proteomics analysis, a total of 2776 proteins were identified for both the monocyte subsets from targets obtained by both QSTAR and LTQ-Orbitrap. A total of 1493 proteins were identified when the criterion of ≥ 2 MS and a relative intensity ratio of < 1.5 for the technical replicates for both platforms and an error factor < 2 for QSTAR only was used. Of 1493 proteins, 455 were differentially expressed at ≥ 1.5 -fold change between the monocyte subsets (Figure 1a). Interestingly, only 27 differential expressed targets were commonly identified from the two platforms (Figure 1b). However, when the differentially expressed transcripts and proteins were mapped into biological processes *in silico* using DAVID,²⁰ Metacore (GeneGo, San Diego, CA, USA) or Ingenuity pathway analysis (IPA, Ingenuity Systems, Inc., Redwood City, CA, USA), they shared many common biological processes (data not shown and Zhao *et al.*²¹) and cell death was one of the major processes identified. When targets related to the cell death process were compared, only two of the targets were common between the two platforms (Figure 1c). The list of differentially expressed transcripts and proteins is available at <http://mendel.bii.a-star.edu.sg/SigN/PKGroup/BloodMonocyte/>.

Differential expression of apoptotic-related transcripts and proteins between monocyte subsets. The list of differentially expressed targets related to apoptosis identified between the two subsets consisted of 56 transcripts and 23

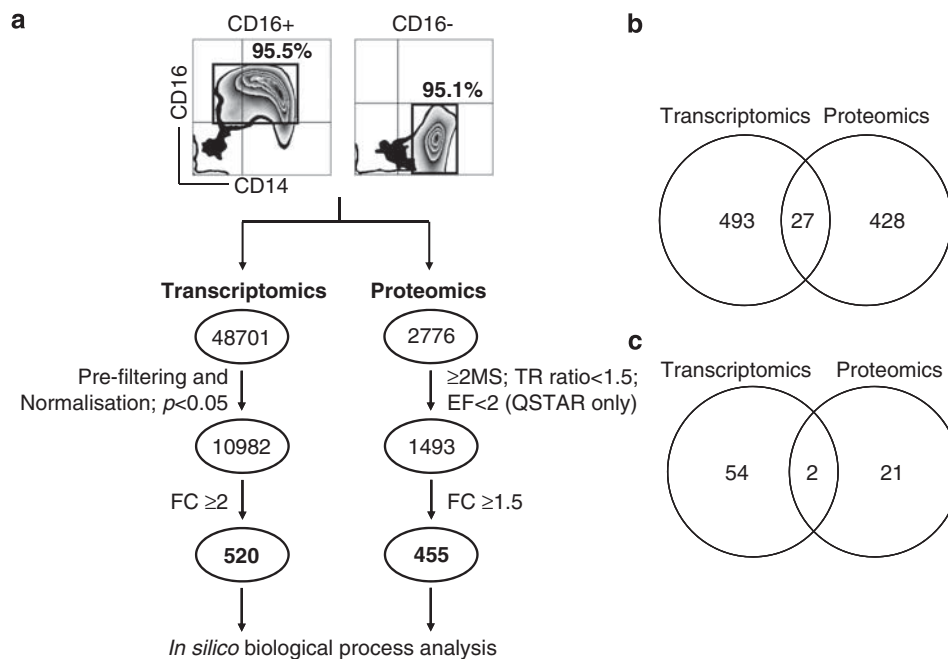


Figure 1 Identification of differentially expressed transcripts and proteins. (a) Flow analyses showing the purity of isolated monocyte subsets using anti-CD14 and anti-CD16 on a FACSCalibur. Percentages indicate purity of the subsets. Plots shown are representative of all isolations. Isolated monocytes are then used for transcriptomic and proteomics, and the flow diagram shows the numbers of transcripts and proteins identified from transcriptomics and proteomics and the statistical criteria leading to the identification of the differentially expressed transcripts and proteins. (b) Venn diagram showing the numbers of total differentially expressed transcripts and proteins that overlapped between the two platforms. (c) Venn diagram showing the numbers of differentially expressed transcripts and proteins related to cell death process that overlapped between the two platforms

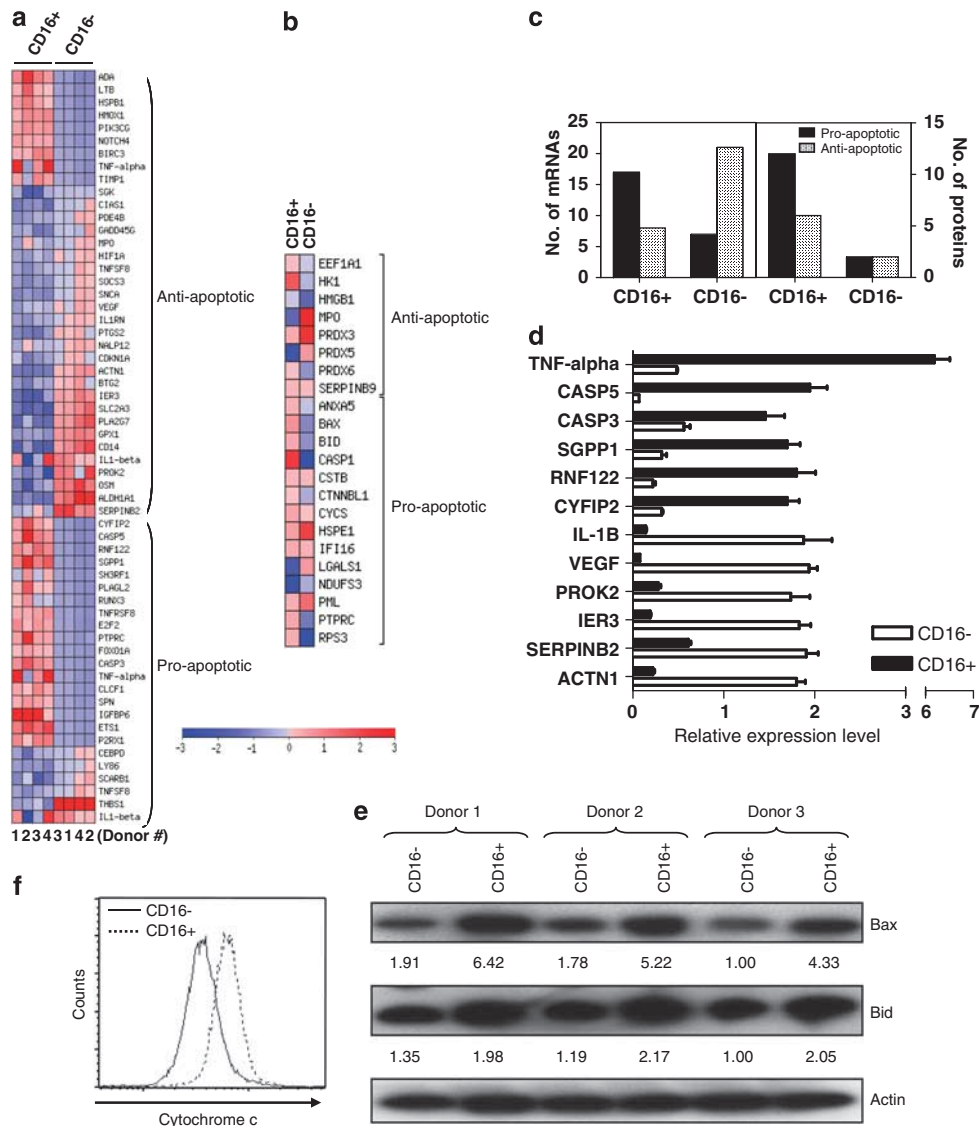


Figure 2 Clustering and validation of apoptotic signatures of monocyte subsets. Supervised clustering of pro- and anti-apoptotic transcripts (a) and proteins (b) using GEPAS. (c) Bar graph representation of the data in panels a and b. Validation of transcriptomics data using real-time PCR (d), and proteomics data using western blot (e) and flow cytometry (f). The numbers below the western blots are relative intensity values after normalizing with actin control. Error bars represent S.E.M. Data shown are from at least three biological replicates that are different from those used in transcriptomics and proteomics experiments. Red and blue color on the scale indicates high- and low-expression intensities, respectively

proteins (Figures 2a and b and Supplementary Tables 1 and 2). Of which, 24 transcripts and 14 proteins had pro-apoptotic functions, 29 transcripts and 8 proteins had anti-apoptotic functions and 3 transcripts and 1 protein had both pro- and anti-apoptotic functions (Supplementary Tables 1 and 2). A large proportion of the transcripts (17 out of 24) and proteins (12 out of 14) with pro-apoptotic functions was expressed at a higher level in CD16+ monocytes. On the other hand, a large proportion of transcripts (21 out of 29) involved in inhibiting apoptosis was more highly expressed in CD16- monocytes (Figure 2c and Supplementary Tables 1 and 2). The relative expression levels of a selection of transcripts (TNF α , CASP5, CASP3, SGPP1, RNF122, CYFIP2, IL-1 β , VEGF, PROK2, immediate early response 3 (IER3), SERPINB2, ACTN1) and proteins (Bax, Bid and cytochrome c) from the

microarray and proteomics data, respectively, were validated using real-time PCR (Figure 2d), western blot (Figure 2e) and flow cytometry (Figure 2f). Validation was performed on samples obtained from three individuals that were different from those used in transcriptomics and proteomics.

CD16+ monocytes exhibit higher spontaneous apoptosis *in vitro*. To examine whether the higher expression of pro-apoptotic genes in CD16+ monocytes reflects a greater tendency to undergo spontaneous apoptosis, isolated monocyte subsets were cultured in serum-supplemented medium, and spontaneous apoptosis was determined using Annexin-V, an indicator of phosphatidylserine exposure during early apoptosis and TO-PRO3, an indicator of membrane damage during late apoptosis. *In vitro* culture

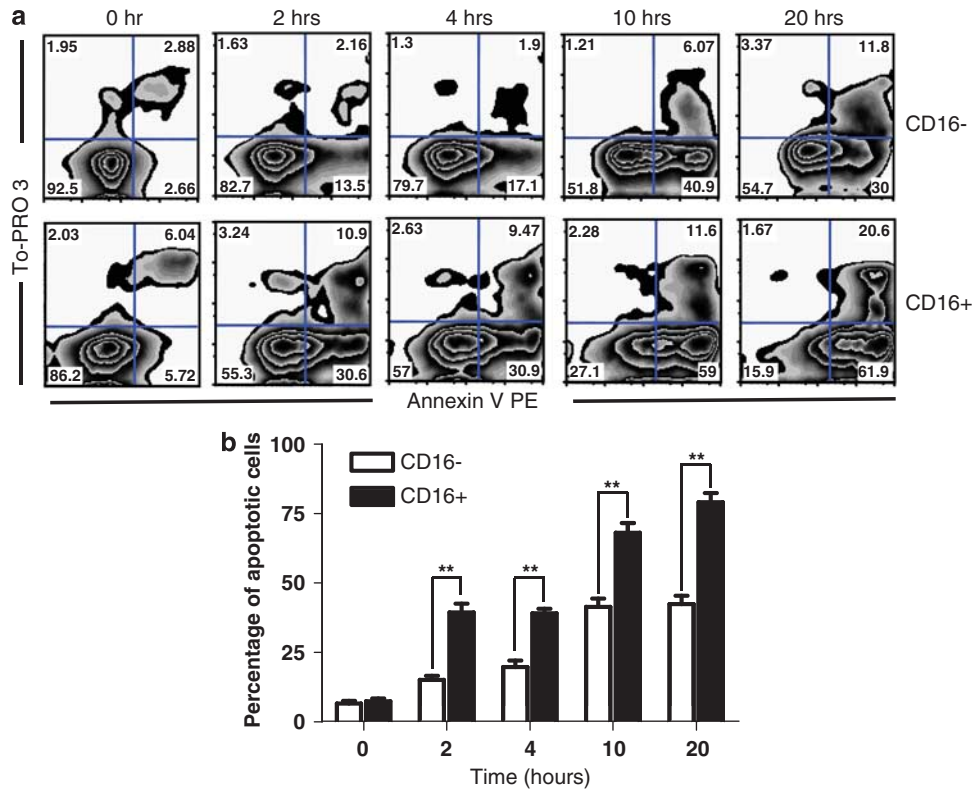


Figure 3 CD16⁺ monocytes exhibited higher spontaneous apoptosis in *in vitro* culture. (a) FACS analysis to assess apoptosis in isolated monocyte subsets with Annexin-V and To-PRO3 after *in vitro* culture for the different time points indicated. Percentages of Annexin-V-positive and Annexin-V/TO-PRO3 double-positive cells with respect to total cells are indicated in the lower-right and upper-right quadrants, respectively. Data are a representative of at least three independent experiments. (b) Bar graph showing the percentages of apoptotic cells, that is, Annexin-V single-positive and Annexin-V/TO-PRO3 double-positive cells in the two monocyte subsets cultured *in vitro* for the indicated time points. Error bars represent S.E.M. and data shown are from at least three biological replicates. ** indicates $P < 0.01$

CD16⁺ monocytes showed a significantly higher percentage of both early and late apoptotic cells as compared with the CD16⁻ subset. A significant difference could be observed as early as 2 h, 30.6 *versus* 13.5% Annexin V-positive cells detected for CD16⁻ and CD16⁺, respectively (Figures 3a and b). The proportion of apoptotic cells in CD16⁺ monocytes accumulated at a faster rate as the cells were cultured for up to 24 h.

To determine the involvement of caspases in apoptosis, monocyte subsets were cultured for 24 h in the presence or absence of a pan-caspase inhibitor, zVAD-fmk. As shown in Figure 4a, zVAD-fmk treatment reduced cell death in both subsets to a similar extent, indicating that both populations are dying through a caspase-dependent pathway. When the activity of downstream caspases were measured in monocyte subsets cultured for either 3 or 6 h, it was observed that CD16⁺ monocytes exhibited significantly higher activities of caspases 3 and 7 (Figure 4b, lower panel). In fact, the basal activities of caspases 3 and 7 were also observed to be significantly higher (Figure 4b, upper panel). Although both subsets undergo spontaneous apoptosis through a caspase-dependent pathway, the pathway is more pronounced in CD16⁺ monocytes.

The caspase-mediated pathway can occur either through the death receptor (extrinsic) pathway or through the mitochondria (intrinsic) pathway. A number of pro-apoptotic proteins like bax, bid and cytochrome *c* identified in our study

are mitochondrial proteins and are associated with apoptosis occurring through the intrinsic pathway. To establish whether the enhanced apoptosis in CD16⁺ monocytes occurs through the intrinsic pathway, mitochondrial membrane permeability (MMP) was assessed. Using a lipophilic, cationic fluorescent dye TMRM, a higher percentage of CD16⁺ monocytes was observed to have depolarized MMP as compared with CD16⁻ monocytes across all time points, including cells before culture (Figure 4c). Similar results were obtained when two other fluorescent dyes, DiOC₆ and JC-1, were used (data not shown). One hallmark on the loss of MMP is the release of cytochrome *c* from the mitochondria into the cytosol. When the cytochrome *c* content in the cytosol of the two subsets was assessed, a greater amount of cytochrome *c* was observed in the cytosolic fraction of the CD16⁺ subset at 6 and 24 h after *in vitro* culture (Figure 4d), indicating that the intrinsic apoptotic pathway is more active in the CD16⁺ subset.

CD16⁺ monocytes are less protected from oxidative stress. GSH metabolism, a biological process related to apoptosis, was identified *in silico* to be differentially regulated in the two subsets. GSH metabolism protects cells from oxidative damage. Four transcripts involved in GSH metabolism, namely GSH peroxidase 1 (GPX1), microsomal GSH S-transferase 1 (MGST1), IER3 and thioredoxin domain-containing protein 1, were observed to be expressed at a lower level in CD16⁺ compared with

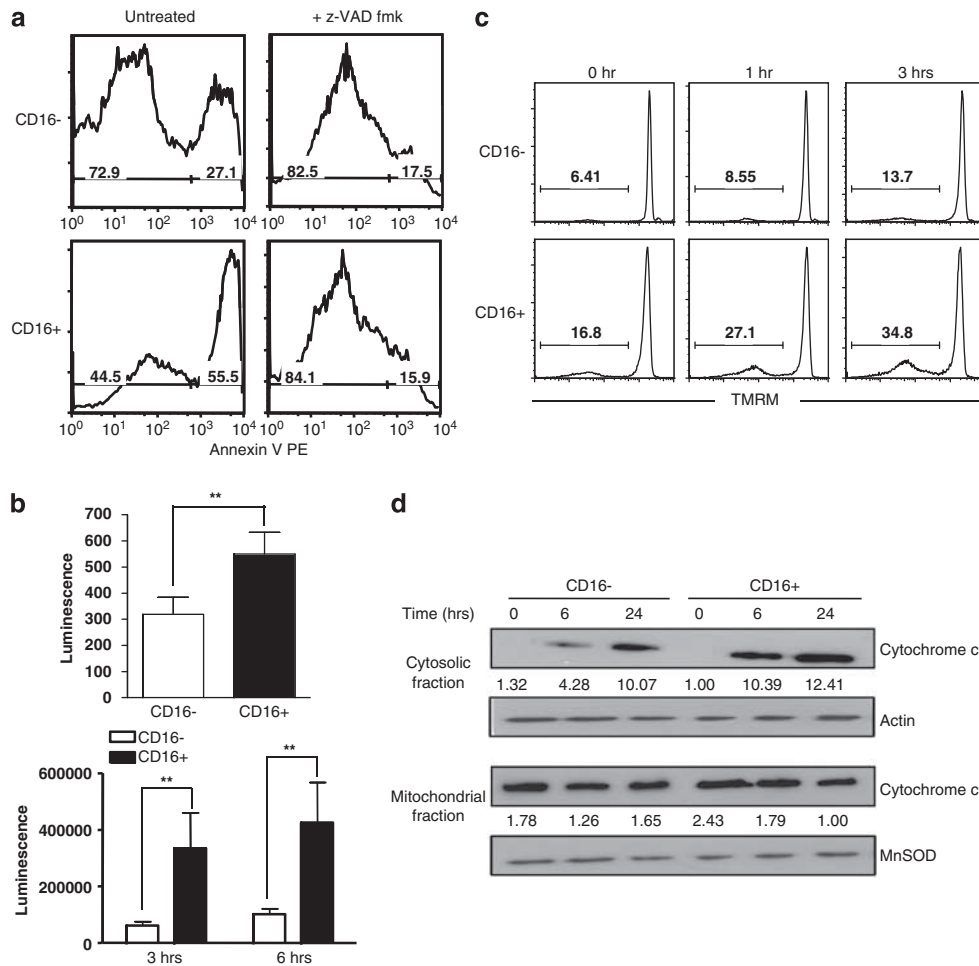
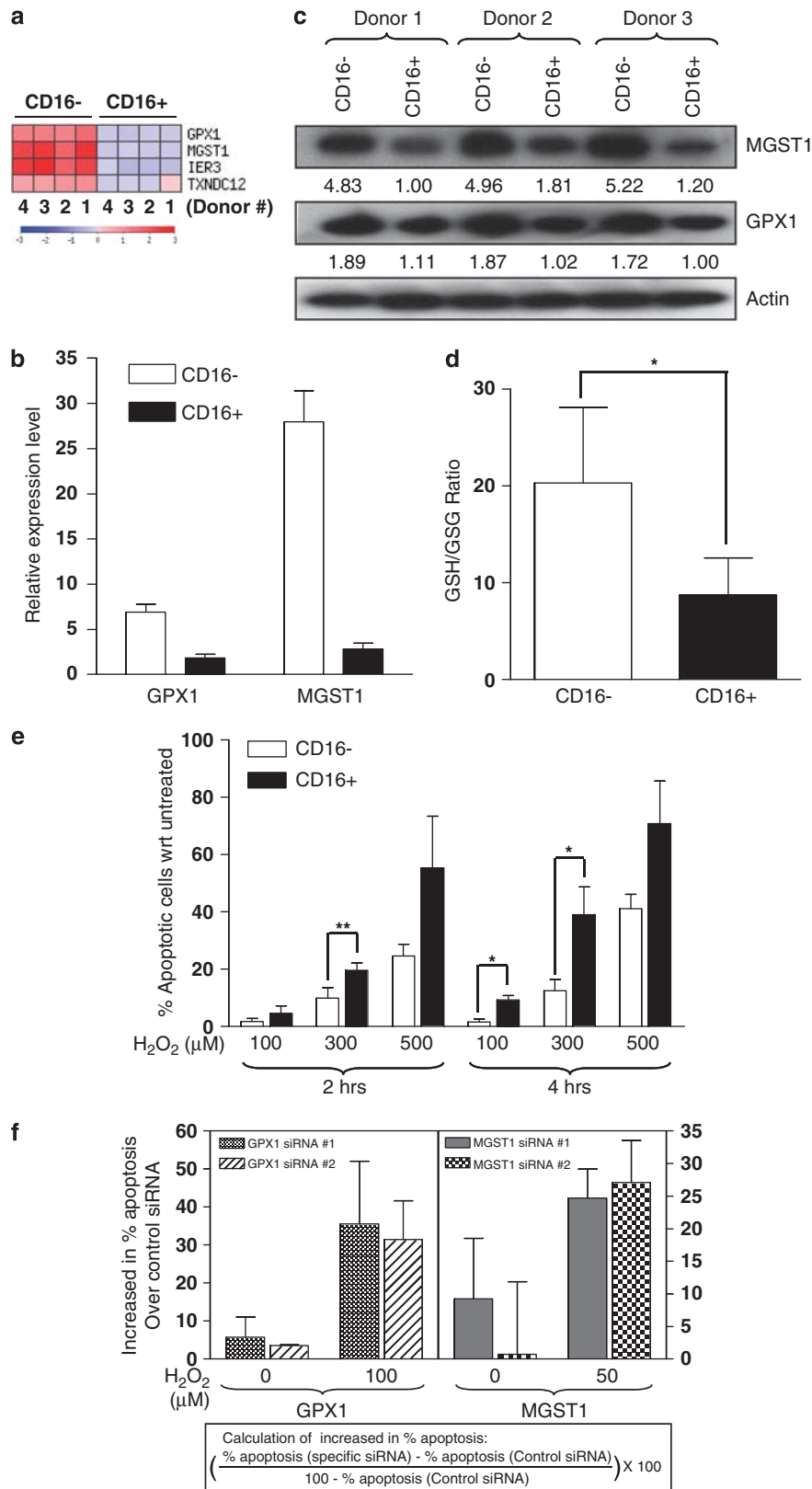


Figure 4 Spontaneous apoptosis is caspase dependent and occurs through the mitochondria. (a) Histogram plots of Annexin-V staining on monocyte subsets after 24 h culture *in vitro* either in the absence or in the presence of z-VAD-fmk. Data are a representative of three independent experiments. (b) Relative caspases 3 and 7 activities in monocyte subsets either freshly isolated (upper panel) or cultured *in vitro* for 3 or 6 h (lower panel). Data are consolidated from at least three independent experiments and error bars represent S.E.M. ** indicates $P < 0.01$. (c) Histogram plots of TMRM fluorescence in isolated monocyte subsets assessed at the various time points on *in vitro* culture. Data are representative of three independent experiments, and numbers indicate the percentage of cells that has reduced TMRM fluorescence with respect to total cells. (d) Western blot analysis of cytochrome c in the cytosolic fraction (upper panel) and mitochondrial fraction (lower panel) isolated from monocyte subsets at the various time points on *in vitro* culture. β -Actin and MnSOD were used as loading controls for cytosolic and mitochondrial fractions, respectively. The numbers below the blots are relative intensity values after normalizing with the respective loading controls. Data shown are representative of four independent experiments

CD16⁻ monocytes (Figure 5a). The differential expressions of GPX1 and MGST1 were validated by both real-time PCR (Figure 5b) and western blot (Figure 5c). To determine whether the lower expression of anti-oxidative genes implicates that CD16⁺ monocytes are in a more oxidized state, levels of reduced GSH versus oxidized GSH (GSSG) were evaluated in both monocyte subsets. Indeed, the GSH/GSSG level was >2-fold lower in CD16⁺ monocytes, indicating that CD16⁺ is in a more oxidized state than CD16⁻ monocytes (Figure 5d). To further investigate whether the lower expression of anti-oxidative genes would render CD16⁺ monocytes more susceptible to oxidant-induced cell death, the two subsets were treated with different concentrations of hydrogen peroxide (H₂O₂) for either 2 or 4 h. On treatment with H₂O₂, CD16⁺ monocytes exhibited a greater percentage of apoptotic cells than did CD16⁻ monocytes under all treatment conditions, indicative of a poorer protection against H₂O₂-induced apoptosis

(Figure 5e). To confirm that the higher expressions of GPX1 and MGST1 in CD16⁻ monocytes are rendering these cells better protection against oxidants, we investigated the susceptibility of these monocytes to 4 h of H₂O₂ treatment after knocking down either GPX1 or MGST1 expression by siRNA. Indeed, the cells became more prone to H₂O₂-induced apoptosis relative to cells transfected with control siRNA (Figure 5f). Similar results were obtained using two different siRNA sequences for each gene target. The efficiency of the knockdown was assessed both at mRNA (Supplementary Figure 2a) and protein levels (Supplementary Figure 2b) 48 h after transfection. This showed that the higher expression of anti-oxidative proteins in CD16⁻ monocytes protected them better against oxidant-induced cell death than CD16⁺ monocytes.

CD16⁺ monocytes exhibit higher rate of aerobic respiration. As CD16⁺ monocytes expressed lower



levels of anti-oxidative genes, we investigated whether they will display higher intracellular levels of oxygen radicals. CD16+ monocytes showed a higher basal level of ROS, as assessed by dichlorofluorescein (DCFH) for general ROS, by dihydroethidine (DHE) for superoxide anions and by 3'-(*p*-aminophenyl) fluorescein (APF) for hydroxyl and hypochlorite radicals (Figure 6a).²²

Interestingly, our proteomics data showed that four proteins involved in aerobic respiration were more abundant in CD16+ monocytes. They were two isoforms of NADH dehydrogenase (NDUFA4 and NDUFS3), cytochrome *c* reductase (UQCRCF) and adenosine 5'-triphosphate (ATP) synthase (ATP5B). These four proteins are components of complexes I, III or V of the respiratory chain within the mitochondria. Aerobic respiration is a metabolic pathway leading to the production of ATP by using energy derived from the transfer of electrons in an electron transport system. During aerobic respiration, electrons may leak from various complexes within the respiratory chain and partially reduce oxygen to superoxide anions, which are the precursors of many ROS. The higher expressions of NDUSF3 and

ATP5B in CD16+ monocytes were validated by western blot (Figure 6b) and corresponded to a greater amount of intracellular ATP detected (Figure 6c). To determine whether ROS originate from the mitochondria as a result of aerobic respiration, MitoSOX was used to detect superoxide in the mitochondria. Indeed, CD16+ monocytes exhibited a higher percentage of MitoSOX-stained cells than did CD16- monocytes both on isolation (0 min) and after *in vitro* culture for 30 min (Figure 6d). These data confirmed that the notably higher superoxide anion levels detected in CD16+ monocytes indeed originated from the mitochondria (Figure 6a). This implies that the higher metabolic activity of CD16+ monocytes resulted in the generation of higher intracellular ROS.

Spontaneous apoptosis of CD16+ monocytes is due to oxidative stress. The higher production of intracellular ROS together with the lower expression of anti-oxidative genes in CD16+ monocytes implies that they may be experiencing oxidative stress. To determine whether the enhanced spontaneous apoptosis in CD16+ monocytes is attributed

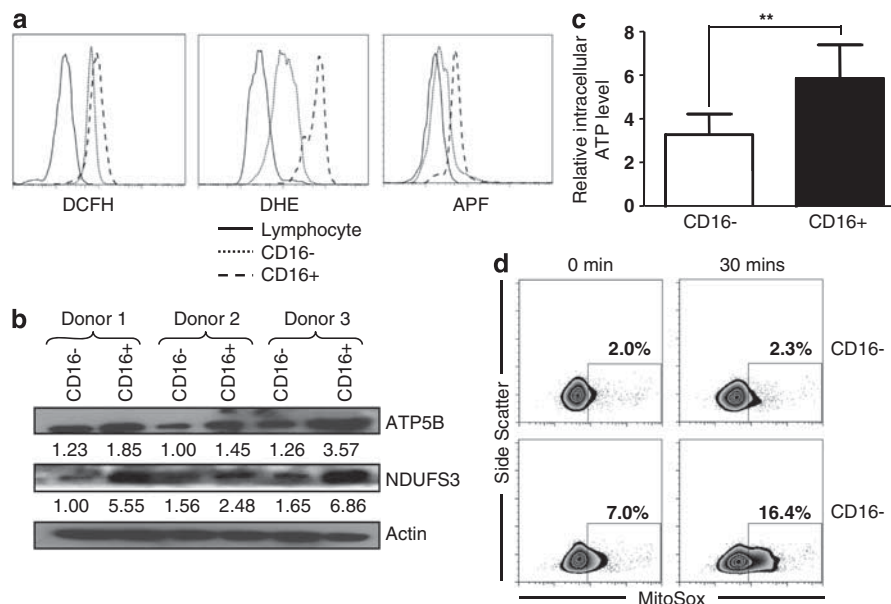


Figure 6 CD16+ monocytes exhibit higher aerobic respiration. (a) Histogram plots showing the intracellular levels of reactive oxygen radicals as measured by DCFH for general ROS, by DHE for superoxide anions and by APF for hydroxyl and hypochlorite radicals in unstimulated lymphocytes (solid line), CD16- (dotted line) and CD16+ (dash line) monocytes. (b) Western blot analysis of ATP5B and NDUFS3 from isolated monocyte subsets from three different individuals to validate the proteomics data. The numbers below the blots are relative intensity values after normalizing with the actin control. (c) Bar graph depicts the intracellular ATP levels in isolated monocyte subsets. (d) FACS analysis using MitoSox to assess mitochondrial superoxide from either freshly isolated monocyte subsets (0 min) or after *in vitro* culture for 30 min. The numbers represent percentages of cells within each box that had intracellular mitochondrial superoxide with respect to total cells. All data shown are from at least three independent experiments and error bars represent S.E.M. ** indicates $P < 0.01$

Figure 5 CD16+ monocytes are less protected from oxidative stress. (a) Supervised clustering of transcripts related to glutathione metabolism based on the normalized expression levels of individual transcripts using GEPAS. Red and blue color on the scale indicates high and low intensities, respectively. Validation of GPX1 and MGST1 expressions in isolated monocyte subsets by real-time PCR (b) and western blotting with β -actin as a loading control (c). The numbers below the western blots are relative intensity values after normalizing with the actin control. (d) Bar graph showing the ratio of GSH (i.e., reduced state) with respect to GSSG (i.e., oxidized state) in isolated monocyte subsets. (e) Bar graph depicts the percentages of apoptotic cells, that is, Annexin-V single-positive and Annexin-V/TO-PRO3 double-positive cells in the isolated monocyte subsets treated for either 2 or 4 h with the indicated concentrations of H_2O_2 with respect to their respective untreated monocyte subsets. (f) Bar graphs indicating the increase in the percentages of apoptotic CD16- monocytes that were either knockdown for GPX1 or MGST1 with respect to cells knockdown with siRNA control that were either left untreated or treated with the indicated concentrations of H_2O_2 for 4 h. Two different siRNA sequences for each target were used. Data are plotted according to the formula as shown. All data shown are from at least three different independent experiments and error bars represent S.E.M. ** indicates $P < 0.01$ and * indicates $P < 0.05$

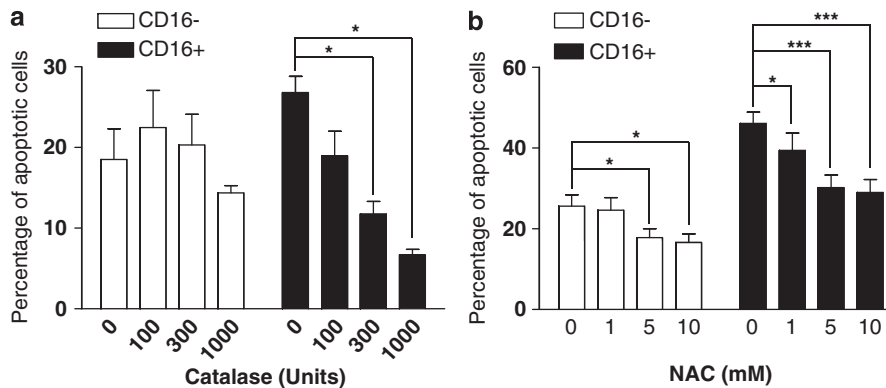


Figure 7 Spontaneous apoptosis in CD16⁺ monocytes is due to oxidative stress. Bar graphs depicting the percentages of apoptotic cells in isolated monocyte subsets cultured either in the absence or presence of various concentrations of catalase for 4 h (a) or NAC for 24 h (b). All data shown are from at least three different independent experiments and error bars represent S.E.M. *** indicates $P < 0.005$ and * indicates $P < 0.05$

to the excess intracellular ROS, the cells were treated with different doses of either *N*-acetyl-cysteine (NAC) or catalase to reduce their oxidative state. NAC is a thiol peptide that replenishes intracellular GSH content,²³ and catalase is an enzyme that catalyzes the hydrolysis of H₂O₂ to water and oxygen. Addition of NAC or catalase resulted in a dose-dependent reduction in the percentage of apoptotic cells in CD16⁺ monocytes (Figures 7a and b), indicating that the higher intracellular ROS level in CD16⁺ monocytes is the cause of their higher apoptotic potential.

Discussion

This study reports the identification of a distinct apoptosis-related gene signature between CD16⁻ and CD16⁺ subsets using combined global transcriptomics and proteomics approaches. CD16⁺ monocytes exhibited a higher propensity to undergo spontaneous apoptosis because of their higher expression of pro-apoptotic genes, lower expression of anti-oxidative genes and higher endogenous ROS levels as a consequence of their greater metabolic activity. Although spontaneous apoptosis of human monocytes is known, this is the first report on a differential spontaneous apoptotic potential of monocyte subsets.

Monocytes are relatively short lived and undergo spontaneous apoptosis in the absence of external survival signals, such as cytokines, microbial products and adherence.^{3,24} When monocytes are treated *in vitro* with proinflammatory mediators such as TNF α , IL-1 β and LPS, their spontaneous apoptosis could be inhibited.^{2,3} *In vivo*, CD16⁺ monocytes were observed to preferentially increase in numbers under numerous inflammatory conditions, such as bacterial sepsis,¹⁶ hemolytic uremic syndrome,²⁵ HIV infection,¹⁷ other acute and chronic infections,²⁶ cardiovascular disease²⁷ and autoimmune disorders.^{18,19} One speculation for the expansion of CD16⁺ monocytes under these pathological conditions is the enhanced survival of this subset. Ellery *et al.* showed both in HIV-infected patients and in an *in vitro* study that HIV preferentially harbored in CD16⁺ monocytes.²⁸ Infected monocytes from HIV patients were found to exhibit an anti-apoptotic gene signature and were less apoptotic²⁰

because they had an increase in Bcl-2/Bax ratio modulated through the mitochondria pathway.²⁹

The Fas–FasL interaction has been implicated in the spontaneous apoptosis of monocytes that mediates through a caspase-dependent mechanism.⁵ Our study shows that the apoptosis of both monocyte subsets were caspase mediated as apoptosis could be inhibited by zVAD-fmk treatment (Figure 4a). However, significantly higher basal caspases 3 and 7 activities were detected in CD16⁺ monocytes, which further increased upon culture *in vitro* (Figure 4b). The higher apoptotic potential of CD16⁺ monocytes could not be mediated through Fas or TRAIL because the expressions of Fas, TRAIL and TRAIL receptors were lower in these cells than CD16⁻ monocytes (Supplementary Figure 3).

Our data indicated that CD16⁺ monocytes spontaneously generated more ROS, which are highly reactive molecules that have the potential to cause cellular damage and apoptosis. ROS-induced apoptosis had been well documented in many cell types, including monocytes.^{5,30} ROS-mediated cell death involves mitochondrial depolarization followed by the subsequent release of mitochondrial pro-apoptotic factors like cytochrome *c*.³¹ We showed in this study that endogenous ROS participated in the enhanced cell death of CD16⁺ monocytes as the reduction of ROS with NAC and catalase could significantly reduce the proportion of apoptotic cells in this subset while having only a minor effect on CD16⁻ monocytes (Figures 7a and b). The source of endogenous ROS, mainly superoxide anions are generated from the mitochondria as a result of higher aerobic respiration in CD16⁺ monocytes. ROS generated from the mitochondria as by-products of aerobic respiration have been widely reported.³² The endogenous ROS, higher abundance of bcl-2 and bax proteins, altered mitochondrial membrane potential and higher cytosolic cytochrome *c* in CD16⁺ monocytes together supported the ROS-dependent cell death mediated through the mitochondria.

Similar to humans, two monocyte subsets have also been described in the mouse.¹³ They are the CX₃CR1^{lo}Gr1⁺ (Gr1⁺) and CX₃CR1^{hi}Gr1⁻ (Gr1⁻) monocytes, widely accepted to be homologous to the human CD16⁻ and CD16⁺ monocytes, respectively.^{12,33} Several studies using CX₃CR1-deficient mice reported that Gr1⁻ monocytes could

not persist in the blood in the absence of signaling through CX₃CR1^{12,14,15} and the expression of the anti-apoptotic gene, Bcl-2 was also greatly reduced in this subset in these mice.^{14,15} When Bcl-2 was overexpressed in CX₃CR1-deficient mice, the numbers of Gr1⁻ monocytes was preferentially restored even though both subsets exhibited comparable transgene levels.¹⁴ Hence, the authors deduced that Gr1⁻ cells are more prone to undergo apoptosis than Gr1⁺ monocytes.¹⁵ The ratio between Bcl-2 and Bax can determine the survival or death of cells.³⁴ Our data showed that CD16⁺ monocytes expressed higher amounts of Bax and Bid than did CD16⁻ monocytes (Figure 2e), but both subsets expressed similar levels of Bcl-2 (Supplementary Figure 4), thereby leading to a lower Bcl-2/Bax ratio, indicative of a more pro-apoptotic phenotype.

Conversely, CD16⁻ monocytes also appeared to be more resistant against oxidative stress as shown by their higher expression of anti-oxidative genes, like GPX1 and MGST1, as compared with CD16⁺ monocytes. GPX1 and MGST1 exhibit GSH peroxidase activities and can potentially protect cells from oxidative damage by lowering intracellular H₂O₂ levels using GSH as the substrate.^{35,36} The knockdown of either GPX1 or MGST1 expression in CD16⁻ monocytes rendered them more susceptible to H₂O₂-induced cell death. There are two possible reasons as to why CD16⁻ monocytes would harness better resistance against oxidative stress. First, we previously reported that CD16⁻ monocytes generate more ROS on encounter with pathogens,²¹ Hence, it is reasonable that they should be better protected against oxidant-mediated cell death. Second, CD16⁻ monocytes express higher levels of G-CSF receptors on their surfaces, and are likely to co-migrate with neutrophils in response to G-CSF to inflammatory sites. At the inflammatory site, they probably function to clear apoptotic neutrophils through their higher expression of phagocytic receptors, such as CD36, C1qR and CD14 to resolve the inflammation (our unpublished data and Zhao *et al.*²¹). In the process, they will also be encountering oxygen radicals produced by activated neutrophils. This differential ability of monocyte subsets to manage oxidative stress is reminiscent to that reported for NK cell subsets, whereby CD56^{bright}CD16⁻ NK subsets were more resistant to oxidant-induced cell death either by exogenous H₂O₂ or by adjacent phagocytic cells, such as activated neutrophils. This was due to their higher anti-oxidative capacity as compared with the CD56^{dim}CD16⁺ NK subset.³⁷

Understanding monocyte apoptosis is of utmost importance under pathological conditions and for the maintenance of homeostasis. CD16⁺ monocytes express higher levels of proinflammatory cytokines such as TNF α and have been termed 'proinflammatory' monocytes (our unpublished data and Belge *et al.*³⁸). We hereby propose that humans develop a self-regulated system through differential apoptosis of monocyte subsets, in which the numbers of proinflammatory CD16⁺ cells are controlled by their pro-apoptotic propensity in the steady state. During an infection, the survival of CD16⁺ monocytes may be enhanced by proinflammatory mediators, so as to enable them to control the infection. However, once the condition is under control and the level of proinflammatory mediators diminishes, CD16⁺ monocytes may die in the

absence of survival signals, bringing the situation back to steady state.² However, the expansion of CD16⁺ monocytes may also be detrimental to the host as the high amount of proinflammatory mediators they produced can result in tissue damage. Hence, a better understanding of the mechanisms involved in the differential apoptotic potential of monocyte subsets will allow us to modulate the enhanced survival of CD16⁺ subsets under pathological conditions in which they contribute to immunopathology and to promote their survival in situations such as infections in which they help to eradicate foreign pathogens.

In conclusion, our data support a model in which CD16⁺ monocytes have a selective sensitivity to ROS-induced apoptosis because of lower anti-oxidative capability and an inherently higher production of endogenous ROS than CD16⁻ monocytes. The intrinsic control of apoptosis of monocyte subsets may represent a mechanism to regulate the CD16⁺ monocyte subset. Further studies using animal models may help to provide a better understanding of the differential apoptotic potential of these monocyte subsets in *in vivo* settings.

Materials and methods

Antibodies. The Abs for flow cytometry are CD16 (3G8) (Biolegend, San Diego, CA, USA), CD14 (61D3) and cytochrome *c* (6H2) (eBioscience, San Diego, CA, USA). The Abs for western blotting are Bid,³⁹ ATP synthase beta (10/ATP), Cytochrome *c* (7H8.2C12), MnSOD (19/MnSOD) (BD, San Diego, CA, USA), Bax (127606), NADH dehydrogenase (17D95) (Santa Cruz Biotechnology, Santa Cruz, CA, USA), GPX1 (Abcam, Cambridge, MA, USA), MGST1 (LS-C36495) (Lifespan Bioscience, Seattle, WA, USA) and Actin (LV1435643) (Millipore, Billerica, MA, USA).

Cells. PBMCs were isolated from buffy coats obtained from Health Sciences Authority (Singapore) using the Ficoll-Hypaque density gradient centrifugation. Isolation of CD16⁻ and CD16⁺ monocyte subsets was performed using the CD16 monocyte isolation kit (Miltenyi Biotec, Bergisch Gladbach, Germany) according to the manufacturer's instructions with some modifications. In brief, after magnetic depletion of NK cells and neutrophils, CD16⁺ monocytes were positively purified using CD16 microbeads. CD16⁻ monocytes were then isolated from the negative fraction with CD14 microbeads. For the isolation of subsets by fluorescence-activated cell sorting (FACS), total monocytes were purified from PBMCs using CD14 microbeads before they were stained with fluorochrome-conjugated anti-CD14 and anti-CD16 Abs and sorted according to the gating shown in Supplementary Figure 1. The purity of the monocyte subsets obtained was examined by flow cytometry with fluorochrome-conjugated anti-CD14 and anti-CD16 Abs. Samples used for experiments other than the proteomics and transcriptomics experiments were obtained from different donors.

Treatments. For apoptosis inhibition, cells were pre-incubated with 20 μ M pan-caspase inhibitor Z-VAD fmk (R&D Systems, Inc., Minneapolis, MN, USA) at 37°C for 24 h. For assessing hydrogen peroxide (H₂O₂)-induced apoptosis, cells were treated with the indicated concentrations of H₂O₂ (Sigma, Saint Louis, MI, USA) for either 2 or 4 h. For inhibition of ROS, cells were treated with catalase (Calbiochem, La Jolla, CA, USA) for 2 h in the absence of serum and with NAC (Calbiochem) for 24 h in the presence of human serum.

Flow cytometry. For cell-surface staining, fluorochrome-conjugated Abs were incubated with cells for 15 min at 4°C. To assess cytochrome *c* levels, intracellular staining was performed using a fixation and permeabilization kit according to the manufacturer's instructions (eBioscience). To assess apoptosis, cells were stained with fluorochrome-conjugated Annexin-V for 15 min at RT and then To-PRO3 was added just before flow cytometry analysis. All data were measured on a FACSCalibur flow cytometer (BD) and analyzed using the FlowJo software (Tree Star Inc., Ashland, OR, USA).

Protein identification and quantitation using Q-STAR or LTQ-Orbitrap MS. Protein identification and quantitation using Q-STAR (Applied Biosystems; MDSSciex) were performed as described previously.²¹ The analysis on the LTQ-Orbitrap MS (ThermoFinnigan, San Jose, CA, USA) was performed as described previously.⁴⁰ In brief, the re-constituted fractions were injected and online desalted in a Zorbax peptide trap (Agilent, Palo Alto, CA, USA). Peptide separation was carried out in a home-packed nanobored C18 column (75 μ m ID \times 15 cm, 5- μ m particles) with a picofrit nanospray tip. The LTQ-Orbitrap was set to perform data acquisition in the positive ion mode, with a selected mass range of 350–2000 *m/z*. The 8 most abundantly charged peptides above a 500-count threshold from each fraction were selected for MS/MS in both pulsed-Q dissociation (PQD) and collision-induced dissociation (CID) and dynamically excluded for 20 s with \pm 5 m.m.u. mass tolerance. The settings for PQD were a Q activation of 0.3, an activation time of 30 ms and a collision energy of 60%, whereas the settings for CID were a Q activation of 0.35, an activation time of 30 ms and a collision energy of 35%.

Peptide quantification and protein identification were achieved by searching the data against the concatenated target-decoy IPI human database using the Mascot server (version 2.2.1). Two missing cleavages were allowed. Precursor ion and MS/MS fragment ion error tolerances were set to <30 p.p.m. and <0.8 Da, respectively. Only peptides with a Mascot score of >30 were taken for protein identification and quantification. For both MS platforms, all proteins reported should have at least two unique peptide matches with iTRAQ ratios, and at least one of the matches should have an expectation value <0.05. The false discovery rate (Decoy) for this search was also <1%.

RNA extraction, real-time PCR, western blotting and transcriptome data analysis. RNA extraction, real-time PCR, western blotting and transcriptome data analysis were all performed as reported previously.²¹ For real-time PCR, primer sequences are available in Supplementary Table 3. Triplicates were set up for each target in every run and results were normalized using the housekeeping gene *18s* rRNA.

In silico biological and functional analyses. Three different approaches were used to explore functional relationships among the differentially expressed mRNA and proteins identified: DAVID (<http://david.abcc.ncifcrf.gov/>), Metacore (GeneGo, https://portal.genego.com/cgi/data_manager.cgi) and IPA (<http://www.ingenuity.com>). The list was input into each of the platforms for identification of biological processes or pathways that differ between the monocyte subsets. Supervised clustering was performed on normalized expression levels of transcripts and proteins using GEPAS (<http://www.gepas.org>).

Caspase 3/7 assay. Up to 2×10^5 cells were added to each well of a 96-well plate and incubated for an appropriate time at 37°C in a 5% CO₂ incubator. The activities of caspase 3/7 were measured using the Caspase-Glo[®] 3/7 assay kit (Promega, Madison, WI, USA) according to the manufacturer's instructions, and luminescence intensity was detected using the GloMax-Multi detection system (Promega).

Measurement of mitochondria membrane potential. Mitochondrial membrane potentials were measured by means of DiOC₆ (Invitrogen, Carlsbad, CA, USA), TMRM or JC-1 (Calbiochem). In brief, 1×10^6 cells per ml were incubated with 20 nM DiOC₆, 200 nM TMRM or 2 μ M JC-1 for 15 min at 37°C before the cells were washed with PBS and analyzed using a flow cytometer.

Isolation of mitochondria and cytosolic fractions. Subcellular fractions were isolated as described previously.³⁹ In all, 3×10^6 cells were cultured for 0, 6 and 24 h and then disrupted using a 271/2-G needle in isolation buffer (200 mM sucrose, 20 μ M EGTA, 5 mM succinate, 2 μ M rotenone, 1 μ g/ml oligomycin, 20 mM Tris, 20 mM HEPES and 1 mM KH₂PO₄, pH 7.2). The cell homogenate was centrifuged at 800 \times g for 10 min at 4°C to remove the nuclei and unbroken cells. The supernatant was centrifuged at 10 000 \times g for 10 min, and the pellet was the 'mitochondrial fraction', whereas the supernatant was further centrifuged at 10 000 \times g for 60 min at 4°C to obtain the 'cytosolic fraction'.

Measurement of intracellular ATP. Intracellular ATP was measured using the ATP bioluminescent assay kit (Sigma) according to the manufacturer's instructions. In brief, the reaction vial was pretreated with 0.1 ml of ATP assay mix solution for 3 min at RT. Next, 0.1 ml of protein lysate from 3×10^6 monocyte

subsets was added quickly into the vial, and the amount of light was immediately measured using a GloMax-Multi detection system. The ATP generated was relative to the total protein concentration.

Measurement of ROS. For ROS measurement, cells were treated with 10 mM of DCFH-diacetate, DHE, APF or MitoSox Red (Invitrogen) for 15 min at 37°C and assessed using a flow cytometer.

siRNA knockdown. The siRNA sequences specific for GPX1 and MGST1, as well as control siRNA were purchased from Invitrogen. Transfection was performed according to the manufacturer's recommendations using lipofectamine 2000 CD reagent (Invitrogen). H₂O₂ treatment, real-time PCR and western blot were performed on cells 48 h after transfection with the respective siRNA.

GSH/GSSG assay. The GSH/GSSG ratio was measured using GSH/GSSG Ratio Assay Kit (Calbiochem) according to the manufacturer's instruction with minor modifications.

Statistical analysis. Data were analyzed for statistical significance either by independent two sample t-test or one-way ANOVA analysis using SPSS (SPSS Inc., Chicago, IL, USA). *P* < 0.05 was considered significant.

Conflict of interest

The authors declare no conflict of interest.

Acknowledgements. We thank Health Sciences Authority (HSA), Singapore, for the supply of buffy coats, the staff of Flow Cytometry and Microarray Units in the Biopolis Shared Facilities, ASTAR for their assistance in cell sorting and samples processing. We also thank Dr. Katja Fink, Dr. Victor Yu and Dr. Han-Kiat Ho for providing reagents and protocols, Dr. Florent Ginhoux, Professor Catharina Svanborg, Dr. Lisa Ng and members of P Kourilsky Laboratory for helpful discussion and critical reading of the manuscript. This research is funded by the Biomedical Research Council, ASTAR, Singapore.

- Whitelaw DM. Observations on human monocyte kinetics after pulse labeling. *Cell Tissue Kinet* 1972; **5**: 311–317.
- Mangan DF, Wahl SM. Differential regulation of human monocyte programmed cell death (apoptosis) by chemotactic factors and pro-inflammatory cytokines. *J Immunol* 1991; **147**: 3408–3412.
- Mangan DF, Welch GR, Wahl SM. Lipopolysaccharide, tumor necrosis factor-alpha, and IL-1 beta prevent programmed cell death (apoptosis) in human peripheral blood monocytes. *J Immunol* 1991; **146**: 1541–1546.
- Kiener PA, Davis PM, Starling GC, Klebanoff SJ, Ledbetter JA et al. Differential induction of apoptosis by Fas-Fas ligand interactions in human monocytes and macrophages. *J Exp Med* 1997; **185**: 1511–1516.
- Um HD, Orenstein JM, Wahl SM. Fas mediates apoptosis in human monocytes by a reactive oxygen intermediate dependent pathway. *J Immunol* 1996; **156**: 3469–3477.
- Kasahara Y, Iwai K, Yachie A, Ohta K, Konno A, Seki H et al. Involvement of reactive oxygen intermediates in spontaneous and CD95 (Fas/APO-1)-mediated apoptosis of neutrophils. *Blood* 1997; **89**: 1748–1753.
- Alexandre J, Batteux F, Nicco C, Chereau C, Laurent A, Guillevin L et al. Accumulation of hydrogen peroxide is an early and crucial step for paclitaxel-induced cancer cell death both *in vitro* and *in vivo*. *Int J Cancer* 2006; **119**: 41–48.
- Ermak N, Lacour B, Druke TB, Vicca S. Role of reactive oxygen species and Bax in oxidized low density lipoprotein-induced apoptosis of human monocytes. *Atherosclerosis* 2008; **200**: 247–256.
- Jacobson MD. Reactive oxygen species and programmed cell death. *Trends Biochem Sci* 1996; **21**: 83–86.
- Tan S, Sagara Y, Liu Y, Maher P, Schubert D. The regulation of reactive oxygen species production during programmed cell death. *J Cell Biol* 1998; **141**: 1423–1432.
- Ziegler-Heitbrock HW. Heterogeneity of human blood monocytes: the CD14+ CD16+ subpopulation. *Immunol Today* 1996; **17**: 424–428.
- Geissmann F, Jung S, Littman DR. Blood monocytes consist of two principal subsets with distinct migratory properties. *Immunity* 2003; **19**: 71–82.
- Gordon S, Taylor PR. Monocyte and macrophage heterogeneity. *Nat Rev Immunol* 2005; **5**: 953–964.
- Jakubzick C, Tacke F, Ginhoux F, Wagers AJ, van Rooijen N, Mack M et al. Blood monocyte subsets differentially give rise to CD103+ and CD103- pulmonary dendritic cell populations. *J Immunol* 2008; **180**: 3019–3027.

15. Landsman L, Bar-On L, Zernecke A, Kim KW, Krauthgamer R, Shagdarsuren E *et al*. CX3CR1 is required for monocyte homeostasis and atherogenesis by promoting cell survival. *Blood* 2009; **113**: 963–972.
16. Fingerle G, Pforte A, Passlick B, Blumenstein M, Strobel M, Ziegler-Heitbrock HW. The novel subset of CD14⁺/CD16⁺ blood monocytes is expanded in sepsis patients. *Blood* 1993; **82**: 3170–3176.
17. Thieblemont N, Weiss L, Sadeghi HM, Estcourt C, Haeffner-Cavaillon N. CD14^{low}CD16^{high}: a cytokine-producing monocyte subset which expands during human immunodeficiency virus infection. *Eur J Immunol* 1995; **25**: 3418–3424.
18. Grip O, Bredberg A, Lindgren S, Henriksson G. Increased subpopulations of CD16⁽⁺⁾ and CD56⁽⁺⁾ blood monocytes in patients with active Crohn's disease. *Inflamm Bowel Dis* 2007; **13**: 566–572.
19. Kawanaka N, Yamamura M, Aita T, Morita Y, Okamoto A, Kawashima M *et al*. CD14⁺, CD16⁺ blood monocytes and joint inflammation in rheumatoid arthritis. *Arthritis Rheum* 2002; **46**: 2578–2586.
20. Giri MS, Nebozyhn M, Raymond A, Gekonge B, Hancock A, Creer S *et al*. Circulating monocytes in HIV-1-infected viremic subjects exhibit an antiapoptosis gene signature and virus- and host-mediated apoptosis resistance. *J Immunol* 2009; **182**: 4459–4470.
21. Zhao C, Zhang H, Wong WC, Sem X, Han H, Ong SM *et al*. Identification of novel functional differences in monocyte subsets using proteomic and transcriptomic methods. *J Proteome Res* 2009; **8**: 4028–4038.
22. Halliwell B, Whiteman M. Measuring reactive species and oxidative damage *in vivo* and in cell culture: how should you do it and what do the results mean? *Br J Pharmacol* 2004; **142**: 231–255.
23. Martinez-Losa M, Cortijo J, Juan G, Ramon M, Sanz MJ, Morcillo EJ. Modulatory effects of N-acetyl-L-cysteine on human eosinophil apoptosis. *Eur Respir J* 2007; **30**: 436–442.
24. Kremer L, Estaquier J, Brandt E, Ameisen JC, Loch C. Mycobacterium bovis Bacillus Calmette Guerin infection prevents apoptosis of resting human monocytes. *Eur J Immunol* 1997; **27**: 2450–2456.
25. Fernandez GC, Ramos MV, Gomez SA, Dran GI, Exeni R, Alduncin M *et al*. Differential expression of function-related antigens on blood monocytes in children with hemolytic uremic syndrome. *J Leukoc Biol* 2005; **78**: 853–861.
26. Nockher WA, Scherberich JE. Expanded CD14⁺ CD16⁺ monocyte subpopulation in patients with acute and chronic infections undergoing hemodialysis. *Infect Immun* 1998; **66**: 2782–2790.
27. Schlitt A, Heine GH, Blankenberg S, Espinola-Klein C, Doppeide JF, Bickel C *et al*. CD14⁺CD16⁺ monocytes in coronary artery disease and their relationship to serum TNF-alpha levels. *Thromb Haemost* 2004; **92**: 419–424.
28. Ellery PJ, Tippett E, Chiu YL, Paukovics G, Cameron PU, Solomon A *et al*. The CD16⁺ monocyte subset is more permissive to infection and preferentially harbors HIV-1 *in vivo*. *J Immunol* 2007; **178**: 6581–6589.
29. Fernandez Larrosa PN, Croci DO, Riva DA, Bibini M, Luzzi R, Saracco M *et al*. Apoptosis resistance in HIV-1 persistently-infected cells is independent of active viral replication and involves modulation of the apoptotic mitochondrial pathway. *Retrovirology* 2008; **5**: 19.
30. Mounjaroen J, Nimmannit U, Callery PS, Wang L, Azad N, Lipipun V *et al*. Reactive oxygen species mediate caspase activation and apoptosis induced by lipoic acid in human lung epithelial cancer cells through Bcl-2 down-regulation. *J Pharmacol Exp Ther* 2006; **319**: 1062–1069.
31. Wang CC, Fang KM, Yang CS, Tzeng SF. Reactive oxygen species-induced cell death of rat primary astrocytes through mitochondria-mediated mechanism. *J Cell Biochem* 2009; **107**: 933–943.
32. Chakraborti T, Das S, Mondal M, Roychoudhury S, Chakraborti S. Oxidant, mitochondria and calcium: an overview. *Cell Signal* 1999; **11**: 77–85.
33. Ingersoll MA, Spanbroek R, Lottaz C, Gautier EL, Frankenberger M, Hoffmann R *et al*. Comparison of gene expression profiles between human and mouse monocyte subsets. *Blood* 2010; **115**: e10–e19.
34. Korsmeyer SJ, Shutter JR, Veis DJ, Merry DE, Oltvai ZN. Bcl-2/Bax: a rheostat that regulates an anti-oxidant pathway and cell death. *Semin Cancer Biol* 1993; **4**: 327–332.
35. Esposito LA, Kokoszka JE, Waymire KG, Cottrell B, MacGregor GR, Wallace DC. Mitochondrial oxidative stress in mice lacking the glutathione peroxidase-1 gene. *Free Radic Biol Med* 2000; **28**: 754–766.
36. Siritantikorn A, Johansson K, Ahlen K, Rinaldi R, Suthiphongchai T, Wlaira P *et al*. Protection of cells from oxidative stress by microsomal glutathione transferase 1. *Biochem Biophys Res Commun* 2007; **355**: 592–596.
37. Thoren FB, Romero AI, Hermodsson S, Hellstrand K. The CD16⁺/CD56^{bright} subset of NK cells is resistant to oxidant-induced cell death. *J Immunol* 2007; **179**: 781–785.
38. Belge KU, Dayyani F, Horelt A, Siedlar M, Frankenberger M, Frankenberger B *et al*. The proinflammatory CD14⁺CD16⁺DR⁺⁺ monocytes are a major source of TNF. *J Immunol* 2002; **168**: 3536–3542.
39. Zhang D, Armstrong JS. Bax and the mitochondrial permeability transition cooperate in the release of cytochrome c during endoplasmic reticulum-stress-induced apoptosis. *Cell Death Differ* 2007; **14**: 703–715.
40. Guo T, Gan CS, Zhang H, Zhu Y, Kon OL, Sze SK. Hybridization of pulsed-Q dissociation and collision-activated dissociation in linear ion trap mass spectrometer for iTRAQ quantitation. *J Proteome Res* 2008; **7**: 4831–4840.



Cell Death and Disease is an open-access journal published by Nature Publishing Group. This work is licensed under the Creative Commons Attribution-NonCommercial-No Derivative Works 3.0 Unported License. To view a copy of this license, visit <http://creativecommons.org/licenses/by-nc-nd/3.0/>

Supplementary Information accompanies the paper on Cell Death and Disease website (<http://www.nature.com/cddis>)